

Observation of Diffractive W -Boson Production at the Fermilab Tevatron

F. Abe,¹⁶ H. Akimoto,³⁵ A. Akopian,³⁰ M. G. Albrow,⁷ S. R. Amendolia,²⁶ D. Amidei,¹⁹ J. Antos,³² S. Aota,³⁵ G. Apollinari,³⁰ T. Asakawa,³⁵ W. Ashmanskas,¹⁷ M. Atac,⁷ F. Azfar,²⁵ P. Azzi-Bacchetta,²⁴ N. Bacchetta,²⁴ W. Badgett,¹⁹ S. Bagdasarov,³⁰ M. W. Bailey,²¹ J. Bao,³⁸ P. de Barbaro,²⁹ A. Barbaro-Galtieri,¹⁷ V. E. Barnes,²⁸ B. A. Barnett,¹⁵ M. Barone,²⁶ E. Barzi,⁹ G. Bauer,¹⁸ T. Baumann,¹¹ F. Bedeschi,²⁶ S. Behrends,³ S. Belforte,²⁶ G. Bellettini,²⁶ J. Bellinger,³⁷ D. Benjamin,³⁴ J. Benlloch,¹⁸ J. Bensinger,³ D. Benton,²⁵ A. Beretvas,⁷ J. P. Berge,⁷ J. Berryhill,⁵ S. Bertolucci,⁹ B. Bevensee,²⁵ A. Bhatti,³⁰ K. Biery,⁷ M. Binkley,⁷ D. Bisello,²⁴ R. E. Blair,¹ C. Blocker,³ A. Bodek,²⁹ W. Bokhari,¹⁸ V. Bolognesi,² G. Bolla,²⁴ D. Bortoletto,²⁸ J. Boudreau,²⁷ L. Breccia,² C. Bromberg,²⁰ N. Bruner,²¹ E. Buckley-Geer,⁷ H. S. Budd,²⁹ K. Burkett,¹⁹ G. Busetto,²⁴ A. Byon-Wagner,⁷ K. L. Byrum,¹ J. Cammerata,¹⁵ C. Campagnari,⁷ M. Campbell,¹⁹ A. Caner,²⁶ W. Carithers,¹⁷ D. Carlsmith,³⁷ A. Castro,²⁴ D. Cauz,²⁶ Y. Cen,²⁹ F. Cervelli,²⁶ P. S. Chang,³² P. T. Chang,³² H. Y. Chao,³² J. Chapman,¹⁹ M.-T. Cheng,³² G. Chiarelli,²⁶ T. Chikamatsu,³⁵ C. N. Chiou,³² L. Christofek,¹³ S. Cihangir,⁷ A. G. Clark,¹⁰ M. Cobal,²⁶ E. Cocca,²⁶ M. Contreras,⁵ J. Conway,³¹ J. Cooper,⁷ M. Cordelli,⁹ C. Couyoumtzelis,¹⁰ D. Crane,¹ D. Cronin-Hennessy,⁶ R. Culbertson,⁵ T. Daniels,¹⁸ F. DeJongh,⁷ S. Delchamps,⁷ S. Dell'Agnello,²⁶ M. Dell'Orso,²⁶ R. Demina,⁷ L. Demortier,³⁰ M. Deninno,² P. F. Derwent,⁷ T. Devlin,³¹ J. R. Dittmann,⁶ S. Donati,²⁶ J. Done,³³ T. Dorigo,²⁴ A. Dunn,¹⁹ N. Eddy,¹⁹ K. Einsweiler,¹⁷ J. E. Elias,⁷ R. Ely,¹⁷ E. Engels, Jr.,²⁷ D. Errede,¹³ S. Errede,¹³ Q. Fan,²⁹ G. Feild,³⁸ C. Ferretti,²⁶ I. Fiori,² B. Flaugher,⁷ G. W. Foster,⁷ M. Franklin,¹¹ M. Frautschi,³⁴ J. Freeman,⁷ J. Friedman,¹⁸ H. Frisch,⁵ Y. Fukui,¹⁶ S. Funaki,³⁵ S. Galeotti,²⁶ M. Gallinaro,²⁴ O. Ganel,³⁴ M. Garcia-Sciveres,¹⁷ A. F. Garfinkel,²⁸ C. Gay,¹¹ S. Geer,⁷ D. W. Gerdes,¹⁵ P. Giannetti,²⁶ N. Giokaris,³⁰ P. Giromini,⁹ G. Giusti,²⁶ L. Gladney,²⁵ D. Glenzinski,¹⁵ M. Gold,²¹ J. Gonzalez,²⁵ A. Gordon,¹¹ A. T. Goshaw,⁶ Y. Gotra,²⁴ K. Goulianos,³⁰ H. Grassmann,²⁶ L. Groer,³¹ C. Grosso-Pilcher,⁵ G. Guillian,¹⁹ R. S. Guo,³² C. Haber,¹⁷ E. Hafen,¹⁸ S. R. Hahn,⁷ R. Hamilton,¹¹ R. Handler,³⁷ R. M. Hans,³⁸ F. Happacher,²⁶ K. Hara,³⁵ A. D. Hardman,²⁸ B. Harral,²⁵ R. M. Harris,⁷ S. A. Hauger,⁶ J. Hauser,⁴ C. Hawk,³¹ E. Hayashi,³⁵ J. Heinrich,²⁵ K. D. Hoffman,²⁸ M. Hohlmann,⁵ C. Holck,²⁵ R. Hollebeek,²⁵ L. Holloway,¹³ A. Hölscher,¹⁴ S. Hong,¹⁹ G. Houk,²⁵ P. Hu,²⁷ B. T. Huffman,²⁷ R. Hughes,²² J. Huston,²⁰ J. Huth,¹¹ J. Hylen,⁷ H. Ikeda,³⁵ M. Incagli,²⁶ J. Incandela,⁷ G. Introzzi,²⁶ J. Iwai,³⁵ Y. Iwata,¹² H. Jensen,⁷ U. Joshi,⁷ R. W. Kadel,¹⁷ E. Kajfasz,²⁴ H. Kambara,¹⁰ T. Kamon,³³ T. Kaneko,³⁵ K. Karr,³⁶ H. Kasha,³⁸ Y. Kato,²³ T. A. Keaffaber,²⁸ L. Keeble,⁹ K. Kelley,¹⁸ R. D. Kennedy,⁷ R. Kephart,⁷ P. Kesten,¹⁷ D. Kestenbaum,¹¹ R. M. Keup,¹³ H. Keutelian,⁷ F. Keyvan,⁴ B. Kharadia,¹³ B. J. Kim,²⁹ D. H. Kim,^{7,*} H. S. Kim,¹⁴ S. B. Kim,¹⁹ S. H. Kim,³⁵ Y. K. Kim,¹⁷ L. Kirsch,³ P. Koehn,²⁹ K. Kondo,³⁵ J. Konigsberg,⁸ S. Kopp,⁵ K. Kordas,¹⁴ A. Korytov,⁸ W. Koska,⁷ E. Kovacs,^{7,*} W. Kowald,⁶ M. Krasberg,¹⁹ J. Kroll,⁷ M. Kruse,²⁹ T. Kuwabara,³⁵ S. E. Kuhlmann,¹ E. Kuns,³¹ A. T. Laasanen,²⁸ S. Lammel,⁷ J. I. Lamoureux,³ T. LeCompte,¹ S. Leone,²⁶ J. D. Lewis,⁷ P. Limon,⁷ M. Lindgren,⁴ T. M. Liss,¹³ N. Lockyer,²⁵ O. Long,²⁵ C. Loomis,³¹ M. Loreti,²⁴ J. Lu,³³ D. Lucchesi,²⁶ P. Lukens,⁷ S. Lusin,³⁷ J. Lys,¹⁷ K. Maeshima,⁷ A. Maghakian,³⁰ P. Maksimovic,¹⁸ M. Mangano,²⁶ J. Mansour,²⁰ M. Mariotti,²⁴ J. P. Marriner,⁷ A. Martin,³⁸ J. A. J. Matthews,²¹ R. Mattingly,¹⁸ P. McIntyre,³³ P. Melese,³⁰ A. Menzione,²⁶ E. Meschi,²⁶ S. Metzler,²⁵ C. Miao,¹⁹ T. Miao,⁷ G. Michail,¹¹ R. Miller,²⁰ H. Minato,³⁵ S. Miscetti,⁹ M. Mishina,¹⁶ H. Mitsushio,³⁵ T. Miyamoto,³⁵ S. Miyashita,³⁵ N. Moggi,²⁶ Y. Morita,¹⁶ J. Mueller,²⁷ A. Mukherjee,⁷ T. Muller,⁴ P. Murat,²⁶ H. Nakada,³⁵ I. Nakano,³⁵ C. Nelson,⁷ D. Neuberger,⁴ C. Newman-Holmes,⁷ C.-Y. Ngan,¹⁸ M. Ninomiya, L. Nodulman,³⁵ S. H. Oh,⁶ K. E. Ohl,³⁸ T. Ohmoto,¹² T. Ohsugi,¹² R. Oishi,³⁵ M. Okabe,³⁵ T. Okusawa,²³ R. Oliveira,²⁵ J. Olsen,³⁷ C. Pagliarone,² R. Paoletti,²⁶ V. Papadimitriou,³⁴ S. P. Pappas,³⁸ N. Parashar,²⁶ S. Park,⁷ A. Parri,⁹ J. Patrick,⁷ G. Pauletta,²⁶ M. Paulini,¹⁷ A. Perazzo,²⁶ L. Pescara,²⁴ M. D. Peters,¹⁷ T. J. Phillips,⁶ G. Piacentino,² M. Pillai,²⁹ K. T. Pitts,⁷ R. Plunkett,⁷ L. Pondrom,³⁷ J. Proudfoot,¹ F. Ptohos,¹¹ G. Punzi,²⁶ K. Ragan,¹⁴ D. Reher,¹⁷ A. Ribon,²⁴ F. Rimondi,² L. Ristori,²⁶ W. J. Robertson,⁶ T. Rodrigo,²⁶ S. Rolli,²⁶ J. Romano,⁵ L. Rosenson,¹⁸ R. Roser,¹³ W. K. Sakumoto,²⁹ D. Saltzberg,⁵ A. Sansoni,⁹ L. Santi,²⁶ H. Sato,³⁵ P. Schlabach,⁷ E. E. Schmidt,⁷ M. P. Schmidt,³⁸ A. Scribano,²⁶ S. Segler,⁷ S. Seidel,²¹ Y. Seiya,³⁵ G. Sganos,¹⁴ M. D. Shapiro,¹⁷ N. M. Shaw,²⁸ Q. Shen,²⁸ P. F. Shepard,²⁷ M. Shimojima,³⁵ M. Shochet,⁵ J. Siegrist,¹⁷ A. Sill,³⁴ P. Sinervo,¹⁴ P. Singh,²⁷ J. Skarha,¹⁵ K. Sliwa,³⁶ F. D. Snider,¹⁵ T. Song,¹⁹ J. Spalding,⁷ T. Speer,¹⁰ P. Sphicas,¹⁸ F. Spinella,²⁶ M. Spiropulu,¹¹ L. Spiegel,⁷ L. Stanco,²⁴ J. Steele,³⁷ A. Stefanini,²⁶ K. Strahl,¹⁴ J. Strait,⁷ R. Ströhmer,^{7,*} D. Stuart,⁷ G. Sullivan,⁵ A. Soumarokov,³² K. Sumorok,¹⁸ J. Suzuki,³⁵ T. Takada,³⁵ T. Takahashi,²³ T. Takano,³⁵ K. Takikawa,³⁵ N. Tamura,¹² B. Tannenbaum,²¹ F. Tartarelli,²⁶ W. Taylor,¹⁴ P. K. Teng,³² Y. Teramoto,²³ S. Tether,¹⁸ D. Theriot,⁷ T. L. Thomas,²¹ R. Thun,¹⁹

M. Timko,³⁶ P. Tipton,²⁹ A. Titov,³⁰ S. Tkaczyk,⁷ D. Toback,⁵ K. Tollefson,²⁹ A. Tollestrup,⁷ W. Trischuk,¹⁴ J. F. de Troconiz,¹¹ S. Truitt,¹⁹ J. Tseng,¹⁸ N. Turini,²⁶ T. Uchida,³⁵ N. Uemura,³⁵ F. Ukegawa,²⁵ G. Unal,²⁵ J. Valls,^{7,*} S. C. van den Brink,²⁷ S. Vejcek III,¹⁹ G. Velev,²⁶ R. Vidal,⁷ M. Vondracek,¹³ D. Vucinic,¹⁸ R. G. Wagner,¹ R. L. Wagner,⁷ J. Wahl,⁵ N. B. Wallace,²⁶ A. M. Walsh,³¹ C. Wang,⁶ C. H. Wang,³² J. Wang,⁵ J. Wang,³² Q. F. Wang,³⁰ A. Warburton,¹⁴ T. Watts,³¹ R. Webb,³³ C. Wei,⁶ C. Wendt,³⁷ H. Wenzel,¹⁷ W. C. Wester III,⁷ A. B. Wicklund,¹ E. Wicklund,⁷ R. Wilkinson,²⁵ H. H. Williams,²⁵ P. Wilson,⁵ B. L. Winer,²² D. Winn,¹⁹ D. Wolinski,¹⁹ J. Wolinski,²⁰ S. Worm,²¹ X. Wu,¹⁰ J. Wyss,²⁴ A. Yagil,⁷ W. Yao,¹⁷ K. Yasuoka,³⁵ Y. Ye,¹⁴ G. P. Yeh,⁷ P. Yeh,³² M. Yin,⁶ J. Yoh,⁷ C. Yosef,²⁰ T. Yoshida,²³ D. Yovanovitch,⁷ I. Yu,⁷ L. Yu,²¹ J. C. Yun,⁷ A. Zanetti,²⁶ F. Zetti,²⁶ L. Zhang,³⁷ W. Zhang,²⁵ and S. Zucchelli²

(CDF Collaboration)

¹Argonne National Laboratory, Argonne, Illinois 60439

²Istituto Nazionale di Fisica Nucleare, University of Bologna, I-40127 Bologna, Italy

³Brandeis University, Waltham, Massachusetts 02264

⁴University of California at Los Angeles, Los Angeles, California 90024

⁵University of Chicago, Chicago, Illinois 60638

⁶Duke University, Durham, North Carolina 28708

⁷Fermi National Accelerator Laboratory, Batavia, Illinois 60510

⁸University of Florida, Gainesville, Florida 60510

⁹Laboratori Nazionali di Frascati, Istituto Nazionale di Fisica Nucleare, I-00044 Frascati, Italy

¹⁰University of Geneva, CH-1211 Geneva 4, Switzerland

¹¹Harvard University, Cambridge, Massachusetts 02138

¹²Hiroshima University, Higashi-Hiroshima 724, Japan

¹³University of Illinois, Urbana, Illinois 61801

¹⁴Institute of Particle Physics, McGill University, Montreal H3A 2T8, and University of Toronto, Toronto M5S 1A7, Canada

¹⁵The Johns Hopkins University, Baltimore, Maryland 21218

¹⁶National Laboratory for High Energy Physics (KEK), Tsukuba, Ibaraki 315, Japan

¹⁷Ernest Orlando Lawrence Berkeley National Laboratory, Berkeley, California 94720

¹⁸Massachusetts Institute of Technology, Cambridge, Massachusetts 02139

¹⁹University of Michigan, Ann Arbor, Michigan 48109

²⁰Michigan State University, East Lansing, Michigan 48824

²¹University of New Mexico, Albuquerque, New Mexico 87132

²²The Ohio State University, Columbus, Ohio 43320

²³Osaka City University, Osaka 588, Japan

²⁴Universita di Padova, Istituto Nazionale di Fisica Nucleare, Sezione di Padova, I-36132 Padova, Italy

²⁵University of Pennsylvania, Philadelphia, Pennsylvania 19104

²⁶Istituto Nazionale di Fisica Nucleare, University and Scuola Normale Superiore of Pisa, I-56100 Pisa, Italy

²⁷University of Pittsburgh, Pittsburgh, Pennsylvania 15270

²⁸Purdue University, West Lafayette, Indiana 47907

²⁹University of Rochester, Rochester, New York 14628

³⁰Rockefeller University, New York, New York 10021

³¹Rutgers University, Piscataway, New Jersey 08854

³²Academia Sinica, Taipei, Taiwan 11530, Republic of China

³³Texas A&M University, College Station, Texas 77843

³⁴Texas Tech University, Lubbock, Texas 79409

³⁵University of Tsukuba, Tsukuba, Ibaraki 315, Japan

³⁶Tufts University, Medford, Massachusetts 02155

³⁷University of Wisconsin, Madison, Wisconsin 53806

³⁸Yale University, New Haven, Connecticut 06511

(Received 14 January 1997)

We report the first observation of diffractively produced W bosons. In a sample of $W \rightarrow e\nu$ events produced in $p\bar{p}$ collisions at $\sqrt{s} = 1.8$ TeV, we find an excess of events with a forward rapidity gap, which is attributed to diffraction. The probability that this excess is consistent with nondiffractive production is 1.1×10^{-4} (3.8σ). The relatively low fraction of $W + \text{jet}$ events observed within this excess implies that mainly quarks from the Pomeron, which mediates diffraction, participate in W production. The diffractive to nondiffractive W production ratio is found to be $R_W = (1.15 \pm 0.55)\%$. [S0031-9007(97)02920-7]

PACS numbers: 13.85.Qk, 12.38.Qk, 12.40.Nn

Approximately 15% of high energy $p\bar{p}$ inelastic collisions are due to single diffraction dissociation, a process in which the incident p or \bar{p} escapes intact losing a fraction $\xi \lesssim 0.1$ of its initial forward momentum. Experiments have shown [1] that the leading role in diffraction is played by the Pomeron [2], which carries the quantum numbers of the vacuum. In QCD the Pomeron is a colorless entity, whose exchange in an event is marked by a ‘‘rapidity gap,’’ i.e., a large region of pseudorapidity [3] devoid of particles.

The partonic structure of the Pomeron was first investigated by the UA8 experiment [4,5], which studied diffractive dijet production at the CERN $S\bar{p}pS$ collider at $\sqrt{s} = 630$ GeV, and more recently by the H1 [6,7] and ZEUS [8,9] experiments in diffractive deep inelastic scattering (DIS) [6–8] and dijet photoproduction [9] in ep collisions at $\sqrt{s} \approx 300$ GeV at HERA. All experiments find that a substantial fraction of the Pomeron structure is ‘‘hard,’’ i.e., consists of partons carrying a large fraction of the Pomeron momentum. From the DIS experiments, which probe directly the quark component of the Pomeron, the hard-quark component is estimated to account for about one-third of the Pomeron momentum. At the Tevatron $\bar{p}p$ collider, a hard-quark Pomeron structure would lead to detectable diffractive W production [10], which to leading order occurs through $q'\bar{q} \rightarrow W$. For a hard-gluon dominated Pomeron, W production can occur through $qg \rightarrow Wq'$, but at a rate lower by order α_s and always in association with a jet.

In this paper, we present the results of a measurement of diffractive W production in $p\bar{p}$ collisions at $\sqrt{s} = 1.8$ TeV using the CDF detector at the Tevatron. Diffraction is tagged by the presence of a rapidity gap in an event

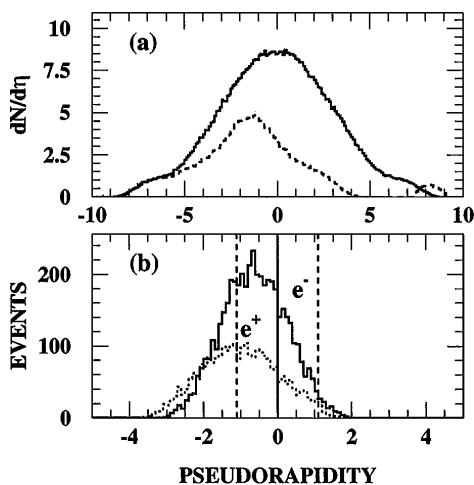


FIG. 1. Monte Carlo generated η distributions: (a) Particle densities for nondiffractive (solid) and for diffractive (dashed) W events for Pomerons of beam momentum fraction $\xi = 0.03$ emitted by protons (at positive η); the small bump at $\eta \approx 8.5$ is due to the leading protons. (b) Electrons and positrons from diffractive $W^\pm (\rightarrow e^\pm \nu)$ events for all Pomerons of $\xi < 0.1$ emitted by protons (the vertical dashed lines define the boundaries of the region of this measurement).

in association with the following expected characteristic features. In a diffractive $W^\pm \rightarrow e^\pm \nu$ event produced in a \bar{p} collision with a Pomeron (\mathcal{P}) emitted by the proton, the rapidity gap is expected to be at positive η (p direction) and the lepton boosted towards negative η (angle-gap correlation). Also, since the Pomeron is quark-flavor symmetric, and since from energy considerations mainly valence quarks from the \bar{p} participate in producing the W , approximately twice as many electrons as positrons are expected (charge-gap correlation). These correlations can be seen in the Monte Carlo (MC) generated distributions of Fig. 1. The opposite correlations are, of course, expected for p - \mathcal{P} collisions with the Pomeron emitted by the \bar{p} . In nondiffractive events, where rapidity gaps may arise from fluctuations in the event particle multiplicity, MC simulations using the PYTHIA [11] program show that there are no significant angle-gap or charge-gap correlations.

We simulate diffractive events using the POMPYPY [12] MC program, which is based on the Ingelman-Schlein model for hard diffraction [13]. The cross section for $p\bar{p} \rightarrow pX$ may be written as

$$\begin{aligned} \frac{d^2 \sigma_{sd}^{p\bar{p}}}{dt d\xi} &= [K \xi^{1-2\alpha(t)} F^2(t)] \sigma_T^{p\bar{p}}(\hat{s}) \\ &= f_{\mathcal{P}/p}(\xi, t) \sigma_T^{p\bar{p}}(\hat{s}), \end{aligned}$$

where K is a constant, ξ is the fraction of the momentum of the proton carried by the Pomeron, t is the square of the four-momentum transfer, $\alpha(t) = 1 + \epsilon + \alpha't$ is the Pomeron trajectory, $F(t)$ is the nucleon form factor, $\hat{s} = \xi s$ is the center of mass energy squared in the \mathcal{P} - \bar{p} reference frame, and $\sigma_T^{p\bar{p}}(\hat{s})$ is the \mathcal{P} - \bar{p} total cross section. This equation suggests the interpretation of single diffraction dissociation as a process in which a flux of Pomerons $f_{\mathcal{P}/p}(\xi, t)$ emitted by the proton interacts with the antiproton. This concept of factorization was extended [13] to hard processes by treating the ‘‘Pomeron flux factor’’ as a flux of particlelike Pomerons with a unique partonic structure. In POMPYPY, the collision of this flux of Pomerons with the nucleon is handled by PYTHIA. All our MC simulations include a simulation of the CDF detector.

The CDF detector is described in detail elsewhere [14,15]. In the rapidity gap analysis we use the ‘‘beam-beam counters’’ (BBC) and the forward electromagnetic (EM) and hadronic (HA) calorimeters. The BBC [14] consist of a square array of 16 scintillation counters on each side of the interaction point covering approximately the region $3.2 < |\eta| < 5.9$. The forward calorimeters cover the region $2.4 < |\eta| < 4.2$ and have projective tower geometry with tower size $\Delta\eta \times \Delta\phi = 0.1 \times 5^\circ$, where ϕ is the azimuthal angle. An energy threshold of 1.5 GeV (sum of EM plus HA energies) is used for each tower to exclude calorimeter noise.

The data sample was obtained during collider runs 1A (1992-1993) and 1B (1994-1995) by triggering on an electron of high transverse momentum $P_T = P \sin \theta_e$,

and on missing transverse energy \cancel{E}_T [16]. We used events with $\cancel{E}_T > 20$ GeV and an isolated [17] electron of $E_T > 20$ GeV in the central region $|\eta| < 1.1$, where the tracks of charged particles can be completely reconstructed. After implementing a cut retaining events with one primary vertex only, 8246 events remained. The one-vertex cut was imposed to exclude events with two interactions in the same beam-beam crossing, since the overlay of a “minimum bias” on a diffractive W event could eliminate the rapidity gap.

We search for a diffractive W signal by analyzing the correlations between the η of the electron η_e or the sign of its charge C_e , and the multiplicity of one or the other of the BBCs. Each event enters into two distributions, one with $\eta_e \eta_{\text{BBC}} < 0$ (angle-correlated) or $C_e \eta_{\text{BBC}} < 0$ (charge-correlated), and the other with $\eta_e \eta_{\text{BBC}} > 0$ (angle-anticorrelated) or $C_e \eta_{\text{BBC}} > 0$ (charge-anticorrelated). A doubly correlated (anticorrelated) distribution is the BBC multiplicity distribution for events with $\eta_e C_e > 0$ and $\eta_e \eta_{\text{BBC}} < 0$ ($\eta_e \eta_{\text{BBC}} > 0$). Figure 2 shows the observed correlations as a function of BBC multiplicity N_{BBC} for events with tower multiplicity N_T less than eight in the forward calorimeter adjacent to a given BBC. The cut on N_T is imposed to reduce the nondiffractive contribution to the signal, since the

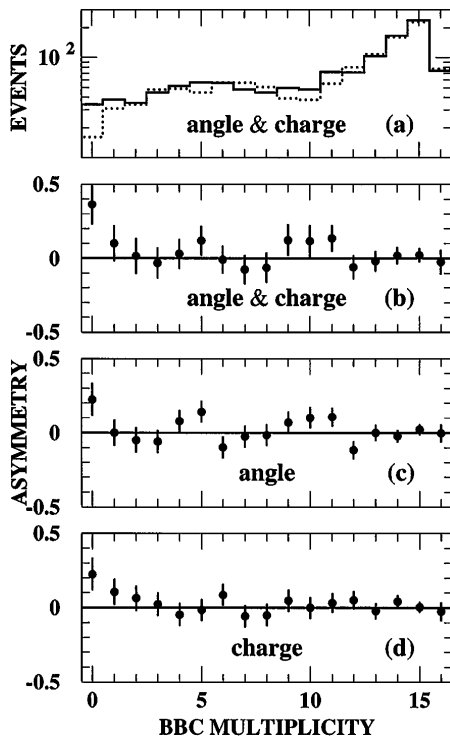


FIG. 2. (a) Electron angle and charge doubly correlated (solid) and anticorrelated (dashed) distributions (see text) versus BBC multiplicity and (b) the corresponding asymmetry, defined as the bin-by-bin difference over sum of the two distributions in (a). The diffractive signal is seen in the first bin as an excess of events in the correlated distribution in (a), and as a positive asymmetry in (b). An asymmetry is also seen in the first bin of the individual angle (c) and charge (d) distributions.

signal is concentrated at low N_{BBC} and is expected to have low N_T as well. Figure 2(a) shows the angle and charge doubly correlated (solid) and doubly anticorrelated (dashed) BBC multiplicities. The peaking at high multiplicities is caused by saturation due to the finite BBC segmentation. The two distributions agree well above the first three bins, but the correlated distribution has an excess in the first bin, consistent with the signature expected from diffractive events with a rapidity gap. This excess can be seen more clearly in Fig. 2(b), which shows the bin-by-bin asymmetry (difference divided by sum) of the two distributions of Fig. 2(a). An excess is also seen in the individual angle [Fig. 2(c)] and charge [Fig. 2(d)] correlated asymmetries, as expected for diffractive production. From MC simulations of nondiffractive W production and using Poisson statistics, the probability that the observed excess in the first bin of both the angle and charge correlated distributions is due to simultaneous fluctuations in the nondiffractive background was estimated to be 1.1×10^{-4} .

The quark to gluon fraction of the partons of the Pomeron participating in W production may be evaluated from the fraction of diffractive $W + \text{jet}$ events observed. Simulations performed with a hard-gluon (quark) Pomeron structure predict the fraction of diffractive W events containing at least one jet with $E_T > 6$ GeV (within an $\eta - \phi$ cone radius of 0.7) to be 0.66 (0.20). For nondiffractive W events with similar kinematics the predicted “jet fraction” is 0.34, consistent with measurements in a nondiffractive data sample. In the first bin of Fig. 2(a) (solid histogram) there are 34 events, among which we estimate 21 to be diffractive and 13 nondiffractive. Multiplying these numbers by the corresponding predicted jet fractions yields an expectation of 18.4 ± 2.8 (8.8 ± 2.5) events with a jet for a hard-gluon (quark) Pomeron structure. The data contain eight events with a jet, which implies that predominantly quarks from the Pomeron participate in W production.

We use the doubly correlated distributions of Fig. 2(a) to evaluate the ratio R of diffractive to nondiffractive W production rates. As a ratio, R is insensitive to lepton selection cuts or inefficiencies and to the uncertainty in the luminosity. The acceptance for diffractive events is obtained from POMPYT using a hard-quark Pomeron structure of the form $\beta G(\beta) = 6\beta(1 - \beta)$, where β is the fraction of the momentum of the Pomeron carried by the quark. In order to check for possible systematic effects due to BBC noise or inefficiencies that could distort the low multiplicity binning and thereby give an incorrect R ratio, we evaluate R using events with a BBC multiplicity upper bound N_B , and we vary N_B from zero to seven. Figure 3(a) shows the resulting R values, and Fig. 3(b) the MC “gap acceptance,” as a function of N_B . The gap acceptance for bin N_B is defined as the fraction of events with $N_{\text{BBC}} \leq N_B$ (the lepton acceptance is not included here). The errors in the points of Fig. 3(a), which are statistical, increase with increasing N_B as more

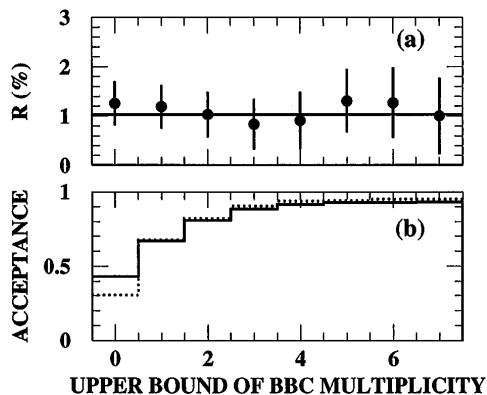


FIG. 3. (a) Diffractive to nondiffractive W production ratio (not corrected for BBC occupancy or one-vertex cut efficiency) as a function of upper bound BBC multiplicity N_B . The solid line passes through the $N_B = 2$ point, which we use as our result; (b) gap acceptance for angle-gap and charge-gap doubly correlated (solid) and anticorrelated (dashed) diffractive events with an electron within $|\eta| < 1.1$.

background is being subtracted. To reduce the sensitivity of the result to the acceptance calculation, we retain as our signal the value $R = (1.03 \pm 0.46)\%$ of the $N_B = 2$ bin, where the acceptance is 81% and varies relatively slowly with N_B .

As a systematic uncertainty in the gap-acceptance calculation we assign $\pm 13\%$, which is one-half of the difference between the acceptances of $N_B = 1$ and $N_B = 3$ divided by the acceptance of $N_B = 2$. In deriving the ratio R we assumed that the nondiffractive contributions to the correlated and anticorrelated distributions in Fig. 2(a) are identical. This assumption is justified by the excellent matching of the two distributions for $N_B > 3$. A possible mismatch of the distributions within the available statistics introduces a systematic uncertainty, which was evaluated as follows. We made a straight line fit to the asymmetry of bins 4–10 of Fig. 2(b), and extrapolated the fit into bins 1–3. For each of the bins 1–3, we multiplied the extrapolated asymmetry and its error by twice the number of anticorrelated events, since the average number of nondiffractive correlated and anticorrelated events is expected to be the same, and added up the results for the three bins. Treating the sum as a signal yields a diffractive to nondiffractive ratio of $(0.01 \pm 0.11)\%$, which is consistent with zero. We treat the error of $\pm 0.11\%$ as a systematic uncertainty in our measured value of R and add it in quadrature to the gap-acceptance uncertainty to obtain a combined systematic uncertainty of $\pm 0.18\%$.

From a study of the rate of W events versus instantaneous luminosity we estimate that a correction of $0.95 \pm 0.05(\text{syst})$ must be applied to R due to the different efficiency of the single vertex cut for diffractive and nondiffractive events. In addition, we apply a correction for the BBC occupancy by particles from a second interaction that does not have a reconstructed vertex. From a study of a sample of 98 000 events recorded by trigger-

ing the detector on beam-beam crossings only, we determined that the probability of finding more than two hits in a BBC is 15%, corresponding to a BBC livetime acceptance of 0.85 by which we divide R . The corrected value for R is $R_W = [1.15 \pm 0.51(\text{stat}) \pm 0.20(\text{syst})]\%$. From MC simulations we estimate that the diffractive events are concentrated at ξ values in the range 0.01–0.05.

Below we compare our results with POMPYT predictions and with results from other experiments. The predictions depend on the assumed Pomeron structure function and on the form and normalization of the Pomeron flux factor $f_{p/p}(\xi, t)$. We first use the “standard” flux factor [18] with parameters $\alpha(t) = 1.115 + 0.26t$ and $K = 0.73 \text{ GeV}^{-2}$; for the nucleon form factor we use [19] $F(t) = (4m_p^2 - 2.8t)(4m_p^2 - t)^{-1}[1 - t/0.7]^{-2}$. For a two (three) flavor hard-quark Pomeron structure of the form $\beta G(\beta) = 6\beta(1 - \beta)$ we obtain $R_W^{hq} = 24\%$ (16%), while for a hard-gluon structure of the same form, $R_W^{hg} = 1.1\%$. Our measured ratio $R_W = (1.15 \pm 0.55)\%$, favors a purely gluonic Pomeron, which, however, is incompatible with the low fraction of diffractive W + jet events we observe. The HERA experiments on DDIS [6,8] at $8.5 < Q^2 < 65 \text{ GeV}^2$ report a quark component in the Pomeron structure which is flat in β , rises slowly with Q^2 at any given fixed β , and accounts for a fraction of about one-third of the momentum of the Pomeron, assuming the standard Pomeron flux. Independent of the Pomeron flux normalization, by combining diffractive dijet photoproduction and DDIS results, the ZEUS Collaboration reports [9] an integrated hard-quark momentum fraction of $0.2 < f_q < 0.7$, while the H1 Collaboration [7], from a QCD analysis of DDIS, obtains $f_q \approx 0.2$ at $Q^2 \sim 60 \text{ GeV}^2$. The Q^2 evolution from $Q^2 = 60 \text{ GeV}^2$ to $Q^2 = M_W^2$ of the Pomeron structure function proposed by H1 does not change significantly the quark component participating in W production. Using a Pomeron with a hard-quark fraction of 0.2 and a gluon fraction of 0.8, POMPYT predicts ratios R_W of 5.7% (4.1%) for two (three) quark flavors, which are larger than our measured value of $(1.15 \pm 0.55)\%$ by more than eight (five) standard deviations.

We now compare our results with POMPYT predictions using the “renormalized” Pomeron flux [18], defined as the standard flux normalized, if its integral exceeds unity, to one Pomeron per nucleon. The normalization factor is ≈ 9 at $\sqrt{s} = 1.8 \text{ TeV}$ (CDF) and ≈ 1 at HERA (see [18]). The predictions for R_W become 2.7% (1.8%) for a two (three) flavor pure hard-quark and 0.12% for a pure hard-gluon Pomeron structure. Based on these predictions, our R_W value of $(1.15 \pm 0.55)\%$ implies hard-quark fractions of $f_q = 0.4 \pm 0.2$ (0.6 ± 0.3) for two (three) quark flavors. These fractions are consistent with the ZEUS and H1 results of $0.2 < f_q < 0.7$ and $f_q \approx 0.2$, respectively. Assuming the momentum sum rule $f_q + f_g = 1$, the predicted fractional gluon contribution to R_W is $(0.12\%)(1 - f_q)/[(0.12\%)(1 - f_q) + Af_q]$, where $A = 2.7\%$ (1.8%)

for two (three) quark flavors. From our values of f_q , the gluon contribution to R_W is predicted to be 6.6% (4.2%) for two (three) quark flavors, which can explain the low fraction of $W + \text{jet}$ events we observe.

In conclusion, we have observed diffractive W production in $p\bar{p}$ collisions at $\sqrt{s} = 1.8$ TeV and measured the ratio of diffractive to nondiffractive production rates to be $R_W = (1.15 \pm 0.55)\%$. The relatively small fraction of diffractive $W + \text{jet}$ events we observe implies that mainly quarks from the Pomeron participate in diffractive W production.

We thank the Fermilab staff and the technical staffs of the participating institutions for their vital contributions. This work was supported by the U.S. Department of Energy and National Science Foundation; the Italian Istituto Nazionale di Fisica Nucleare; the Ministry of Education, Science and Culture of Japan; the Natural Sciences and Engineering Research Council of Canada; the National Science Council of the Republic of China; and the A. P. Sloan Foundation.

*Visitor.

- [1] K. Goulianos, Phys. Rep. **101**, 169 (1983).
- [2] P.D.B. Collins, *An Introduction to Regge Theory and High Energy Physics* (Cambridge University Press, Cambridge, England, 1977).
- [3] We use rapidity and pseudorapidity η interchangeably; $\eta \equiv -\ln(\tan \frac{\theta}{2})$, where θ is the polar angle of a particle with respect to the proton beam direction.
- [4] R. Bonino *et al.*, Phys. Lett. B **211**, 239 (1988).
- [5] A. Brandt *et al.*, Phys. Lett. B **297**, 417 (1992).
- [6] T. Ahmed *et al.*, Phys. Lett. B **348**, 681 (1995).
- [7] H1 Collaboration, C. Adloff *et al.*, in Proceedings of the International Conference on High Energy Physics, Warsaw, Poland, July 1996 (to be published); H1 Collaboration, J.P. Phillips *et al.*, *ibid.*
- [8] M. Derrick *et al.*, Z. Phys. C **68**, 569 (1995).
- [9] M. Derrick *et al.*, Phys. Lett. B **356**, 129 (1995).
- [10] P. Bruni and G. Ingelman, Phys. Lett. B **311**, 317 (1993).
- [11] T. Sjöstrand, Comput. Phys. Commun. **82**, 74 (1994).
- [12] P. Bruni and G. Ingelman, Report No. DESY-93-187; in *Proceedings of the International Europhysics Conference on High Energy Physics, Marseille, France, 1993*, edited by J. Carr and M. Perrottet (Editions Frontières, Gif-sur-Yvette, France, 1994), p. 595.
- [13] G. Ingelman and P. Schlein, Phys. Lett. B **152**, 256 (1985).
- [14] F. Abe *et al.*, Nucl. Instrum. Methods Phys. Res., Sect. A **271**, 387 (1988).
- [15] D. Amidei *et al.*, Nucl. Instrum. Methods Phys. Res., Sect. A **350**, 73 (1994).
- [16] The transverse energy E_T measured by a calorimeter cell located at polar angle θ is defined as $E \sin \theta$. Missing E_T , \cancel{E}_T , is defined as the magnitude of the vector that balances the vector sum of E_T in all calorimeter cells within $|\eta| < 3.6$.
- [17] The calorimetric isolation I_{cal} is defined as the sum- E_T in the towers within a cone of radius $r = \sqrt{(\Delta\eta)^2 + (\Delta\phi)^2} = 0.4$ centered on the electron, excluding the E_T of the electron. The "isolated electron" requirement is $I_{cal}/E_T^e < 0.1$.
- [18] K. Goulianos, Phys. Lett. B **358**, 379 (1995).
- [19] A. Donnachie and P. V. Landshoff, Nucl. Phys. B **303**, 634 (1988).